International Journal of Electrical, Electronic and Communication Sciences
ISSN: 2517-9438
Vol:9, No:8, 2015

Broadband Baseband Impedance Control for Linearity Enhancement in Microwave Devices

Muhammad Akmal Chaudhary

***Abstract*—**The out-of-band impedance environment is considered to be of paramount importance in engineering the in-band impedance environment. Presenting the frequency independent and constant out-of-band impedances across the wide modulation bandwidth is extremely important for reliable device characterization for future wireless systems. This paper presents an out-of-band impedance optimization scheme based on simultaneous engineering of significant baseband components IF1 (twice the modulation frequency) and IF2 (four times the modulation frequency) and higher baseband components such as IF3 (six times the modulation frequency) and IF4 (eight times the modulation frequency) to engineer the in-band impedance environment. The investigations were carried out on a 10W GaN HEMT device driven to deliver a peak envelope power of approximately 40.5dBm under modulated excitation. The presentation of frequency independent baseband impedances to all the significant baseband components whilst maintaining the optimum termination for fundamental tones as well as reactive termination for 2nd harmonic under class-J mode of operation has outlined separate optimum impedances for best intermodulation (IM) linearity.

***Keywords*—**Active load-pull, baseband, device characterisation, waveform measurements.

I. Introduction

THE advent of 4th generation communication systems has led to probe the power device related inherent non-linearity to meet the stringent spectral efficiency requirements. A major obstacle in achieving the linearity specifications is bandwidth dependent distortion effects, otherwise called memory effects. It is widely reported that electrical memory effects are caused by baseband, fundamental as well as 2nd harmonic impedance variation as a function of modulation frequency. The interest here is mainly in the 2nd order non-linearity that causes components to mix to create the inter-modulation distortion (IMD) from the baseband and 2nd harmonic band. The 2nd order non-linearities can be controlled by manipulating the impedances presented to these frequency bands [1]-[5]. In general, the in-band distortion effects cannot be reduced by filtering because they are close in frequency to the fundamental signal. Additionally, the reduction of IMD through simple pre-distortion linearization can become rather difficult when the side-bands become asymmetrical, since the simple pre-distorter assumes symmetrical IMD characteristics according to tone spacing.

With the increasing signal bandwidth and peak-to-average ratio (PAR) associated with modern wireless communication standards; it is frequently observed that predistortion linearization becomes very power amplifier (PA) dependent and modulation standard specific [6]. In addition, when PAs are driven strongly into compression, pre-distortion algorithms have difficulty in capturing the true compression characteristics of the PA because of increased memory effects [6]. This raises an interesting aspect of understanding these anomalous bandwidth dependent memory effects in order to compensate for them. An alternative linearization approach [7] uses the out of-band components to control the in-band distortion, because of their distance from the fundamental signals.

The first part of this paper focuses on the reduction of baseband electrical memory effects which are notoriously difficult to keep constant in a practical design through the application of active IF load-pull by terminating the baseband impedance into ideal short circuits: an impedance environment that would result from conventional design and the use of video bypass capacitors. Further lists the attempts made to linearize the device by considering alternative baseband impedance conditions. As expected, for the Cree GaN device considered [7], the measured linearity significantly improves when negative baseband impedances are presented.

The second part of this paper demonstrates the emulation of a modulated class-J mode of operation by engineering RF loads through modulated RF active load-pull. This has been done to investigate the effectiveness of baseband linearizing technique in improving PA linearity when the fundamental and reactive harmonic loads presented to the device become highly reactive. It is important to mention that 'negative' baseband impedances are non-realisable using conventional passive designs; however, this is not the case when active baseband injection architectures such as Envelope Tracking (ET) are considered.

II. Enhanced Measurement System

In order to characterize and understand the bandwidth dependent electrical memory effects, the measurement system has been demonstrated in [8]-[12] which is capable of presenting the baseband impedance to the two most significant baseband components (IF1 and IF2), generated as a result of 2-tone excitation when the device is driven relatively in its linear region, 1dB below 1dB compression point. This was achieved by combining two, phase coherent arbitrary waveform generators (AWGs) whilst the device was driven at a relatively backed-off level; 1dB below the 1dB compression point. However, when the device is driven more deeply into compression, significantly more mixing terms are generated.

Muhammad Akmal Chaudhary is with department of Electrical Engineering, College of Engineering, Ajman University of Science and Technology, Ajman, United Arab Emirates (e-mail: m.akmal@ajman.ac.ae).

In order to achieve a sufficiently broadband IF termination, a significant modification of the baseband load-pull measurement system was required in order to accurately account for higher baseband components such as IF3 (six times the modulation frequency) and IF4 (eight times the modulation frequency).

A. Multi-Tone Measurement Technique

When measuring complex modulated signals for the applications presented in this paper, it becomes critical to capture detailed features, both in the individual RF cycles, and the modulated RF envelopes, which can be difficult to achieve using sampling oscilloscopes where the number of horizontal points is limited. Folded and interleaved sub-sampling techniques have been developed and effectively compress the spectra of the captured waveforms, and reduce the number of RF cycles per cycle of modulation. Whilst these maintain the integrity of the captured signal [13], [14], they were found to be problematic for capturing complex modulations. In order to capture multi-tone signals using a standard sampling approach, the high-accuracy trigger was provided at the repetition rate of the modulated sequence.

The DSA8000 has only 4000 measurement points making it impractical to capture, in one waveform, all of the relevant information present in a complex multi-sine modulation, so, a new technique was introduced that allowed the sequential capture of 'sections' of a complete modulation cycle, referred to here as “windowing”. In this approach, the oscilloscope is caused to repeatedly trigger at a specific points within the modulation cycle, and by varying precisely the trigger delay and record length, it is possible to isolate and average specific parts of even complex modulation envelopes. Thus, it is possible to step through the modulated waveform, and accurately capture one complete modulation cycle in sufficient detail and accuracy for meaningful analysis. Each captured, 4000 point window is typically averaged 500 times before being downloaded to a computer ready for assembly and analysis. The formulation given in (1) defines the number of windows (W) required to capture one complete cycle of modulation. In the equation, H is the number of required harmonics, f_c is carrier frequency, f_m is modulation frequency and *P* is number of points used, here limited to 4000.

$$W = (2 \times (H + 1) \times f_c) / P \times f_m \quad (1)$$

As well as improving dynamic range, this technique has allowed measurement time to be dramatically reduced - for example, it now takes less than 1 minute to completely capture a device’s non-linear response (including baseband and five harmonics) to a 1MHz modulated 2GHz carrier.

B. Broadband Active RF and IF Load-Pull

Achieving broadband, baseband load emulation, required significant modification to the active load-pull architecture to account for the presence of higher baseband harmonics [15]-[17]. This functionality was achieved in the time domain through the addition of a phase synchronized 80 MHz arbitrary waveform generator (AWG). The generated waveforms comprise frequency components that are multiples of the baseband fundamental frequency, and by controlling the relative magnitude and phase of these, constant and specific baseband impedance scenarios can be presented to a device and maintained across a wide bandwidth. The resulting waveforms are fed directly to the output of the device through a 200W baseband power amplifier, increasing the signal amplitude to the levels required for load-pull. The RF synthesizer used in the modulated waveform measurement system depicted in Fig. 1 is a two-channel Tektronix AWG7000 Arbitrary Waveform Generator. Its two independent yet coherent channels have been used here to synthesize both the modulated fundamental excitation and the complete modulated RF load-pull signal (comprising both fundamental band and harmonic band components) simultaneously, in the time domain [18], [19]. Through the addition of this instrument, the waveform measurement system is able to maintain independent and constant impedance control for each individual tone present across both IF and RF impedance environments, and over a wide modulation bandwidth.

The enhanced modulated waveform measurement system depicted in Fig. 1 has been demonstrated in the first instance using wideband multi-sine stimuli to investigate the bandwidth dependent behaviour of a CREE CGH40010 10W GaN HEMT device.

III. Measurements and Linearity Investigations

All the measurements presented in this section are for a CREE CGH40010 discrete 10W GaN HEMT device, characterized at the center frequency of 2GHz, within a custom 50Ω test fixture. This fixture was calibrated over a relatively wide 50 MHz baseband bandwidth, and over 100 MHz RF bandwidths centered around fundamental, second and third harmonics, with both baseband and RF calibrated reference planes established at the device's package plane. This allowed the accurate and absolute measurement of all the significant voltage and current spectra generated at the input and output of the device.

Two-tone measurements were performed using a 2MHz tone spacing, with the device class-AB biased. The drain voltage used was 28V and a gate voltage was -2.05V, resulting in a quiescent drain current of 250mA. The device was driven into approximately 1.5dB of compression whilst delivering 40.1dBm output peak envelope power (PEP) with fundamental and harmonic components passively terminated into a nominal impedance of 50Ω, at both the input and the output. Active IF load-pull was then used to synthesize a range of IF reflection coefficients in order to quantify the effects of the low frequency, broad-band IF load impedance termination on the non-linear behaviour of the DUT. Fig. 2 illustrates a measurement where the phase of the IF1, IF2 and IF3 loads were varied simultaneously, in steps of 15° around the perimeter of the Smith chart, whilst keeping the magnitude of IF reflection coefficient at unity.

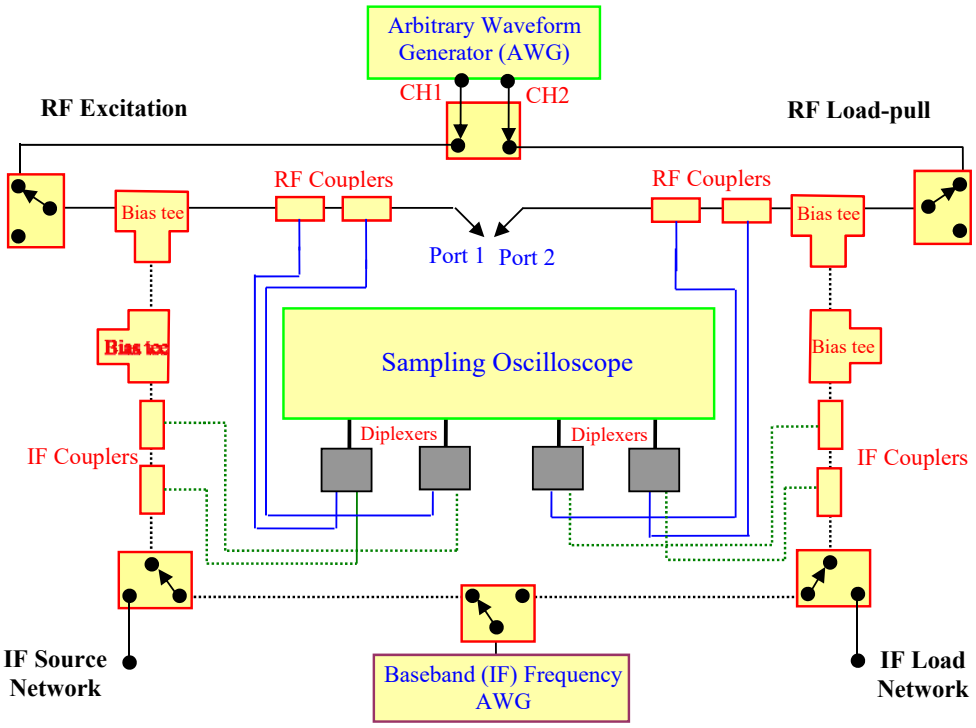

Fig. 1 Multi-tone waveform measurement system with IF and RF test sets

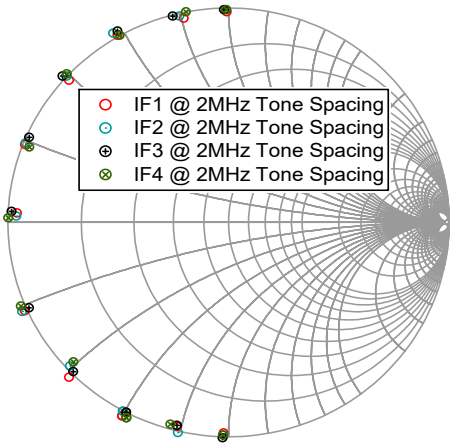

Fig. 2 Experimentally measured baseband impedances at 2MHz tone spacing using active IF load-pull with RF terminated to 50Ω

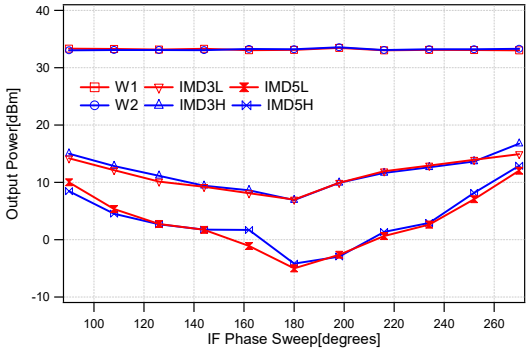

Fig. 3 Experimentally measured IM3 and IM5 linearity as a function of baseband reflection coefficient (Γ_L) for two-tone modulated stimulus

As expected, the results depicted in Fig. 3 clearly show that there exists a strong dependence of IM3 and IM5 magnitude on the phase of the baseband impedance. The results explicitly identify an expected optimum phase in the region of 180° for IF1, IF2 and IF3 loads, where IM3 and IM5 distortion products are minimized.

The measured inter-modulation distortion products presented in Fig. 3 show that when a perfect short impedance ($\Gamma_{IF} = 1\angle 180°$) is presented to the significant baseband components, the measured IM3 and IM5 magnitudes can be seen to be -24dBC and -38dBC respectively.

Active baseband load-pull however has an important advantage in that it is able to seamlessly synthesize both positive baseband impedances within the Smith chart, as well as negative impedances outside the Smith chart.

In order to explore further the optimum baseband impedances for the best linearity conditions, the broadband IF impedance was swept over a measurement grid, including the short circuit condition, and extending some distance outside the Smith chart.

$IM3_L$ and $IM5_L$ contours were then plotted and are shown in Figs. 4 and 5 respectively, and show in both cases, a purely resistive negative optimum impedance. The optimum $IM3_L$ performance (point B) is found to be -43.5dBc, and is approximately 19.5dBc better than the case where usual short

circuit is provided to all the significant baseband components (point A).

With regard to the $IM5_L$ and $IM5_H$, an improvement of 17dBc was achieved at an optimum termination (point C) as compared to the short circuit case (point A). As the contours for $IM3_L$ and $IM3_H$ were found to be almost identical, as was the case for $IM5_L$ and $IM5_H$, only $IM3_L$ and $IM5_L$ contours are presented here.

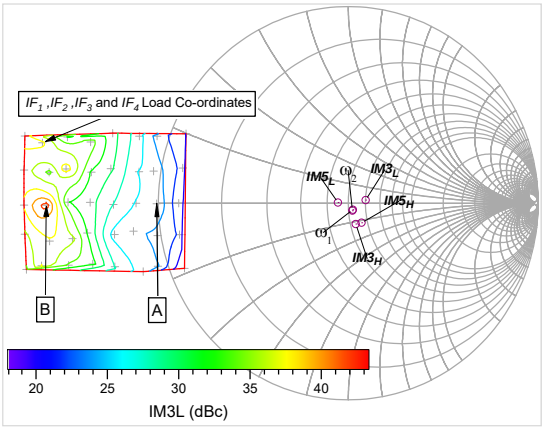

Fig. 4 Experimentally measured IM3L linearity contours as a function of IF1, IF2, IF3 and IF4 loads for two-tone modulated stimulus

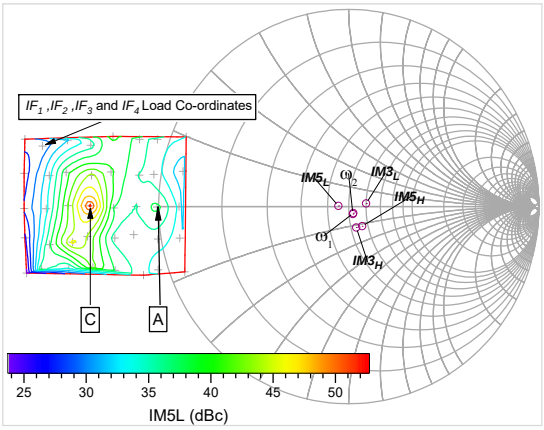

Fig. 5 Experimentally measured IM5L linearity contours as a function of IF1, IF2, IF3 and IF4 loads for two-tone modulated stimulus

If we consider the behaviour of IM3 and IM5 components for the cases of IF loads only located along the real axis, it can be seen that with regard to Fig. 6, the real baseband impedances required to minimize IM3 and IM5 are different, located at points B and C respectively. Establishing the broadband IF load at point B leads to an approximate 11 dB degradation in the established IM5 optimum. Conversely, fixing the IF load at point C results in an approximate 7dB degradation from the established IM3 optimum. Either way, it can be seen that adopting a broadband IF load impedance between points B and C offers a significant improvement in linearity when compared to the usual short circuit termination located at point-A. This technique has been demonstrated at the system level and linearity performance is presented in [7] under two-tone modulated excitation, termed as an auxiliary envelope tracking (AET) by the authors.

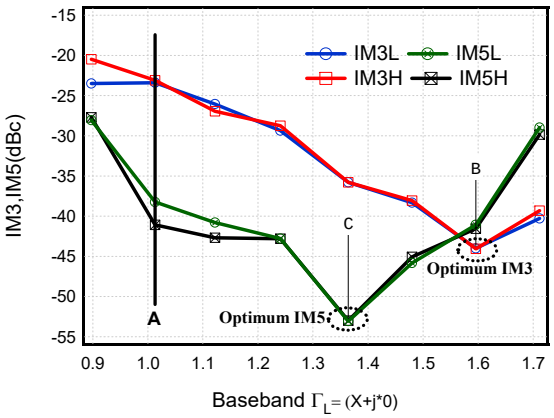

Fig. 6 Experimentally measured IM3 and IM5 linearity trade-off as a function of baseband reflection coefficient (Γ_L)

Fig. 7 shows the baseband voltage waveforms that result when the IF impedances for point B and C are presented to the device.

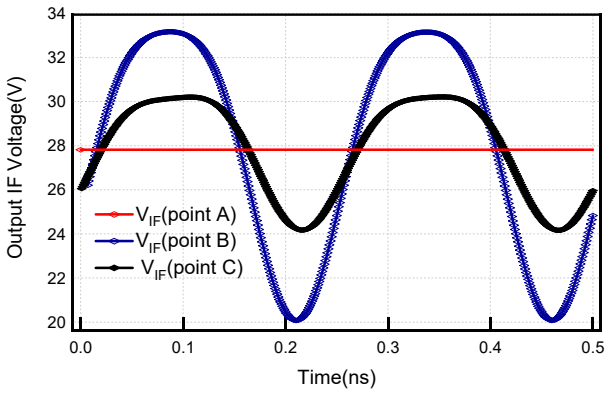

Fig. 7 Experimentally measured baseband voltage that result for the three cases of IF load impedances for minimum IM3 and IM5

IV. Application Focused Measurements

From the results of the previous measurement, it is clear that the optimum baseband impedance for two tone stimulus resides outside the Smith chart. Further 'probing' measurements were carried out whilst varying the drain voltage under a symmetrical 3-tone signal centered at 2 GHz, resulting in 100% amplitude modulation (AM) with an envelope frequency of 2 MHz to confirm that the optimum baseband impedance is not necessarily 'zero'. The device was biased deeply into class AB mode and driven approximately 2.5dB into compression with fundamental and harmonic components terminated into a passive 50Ω load.

The baseband loads were moved on the earlier identified

baseband Γ_L axis. The first IF load condition was a short circuit ($\Gamma_L=1\angle 180^0$) termination to all the four baseband harmonics resulting in an almost static Vds=28V(slight variation are associated with IF5 which was very low and difficult to control). The second IF load condition, for the Vds=24V case, was to increase all four IF components up to 8Vp-p whilst keeping the load purely resistive on the negative axis. For the third IF load condition, the Vds was set to 20V, and the IF components were increased up to 16Vp-p. Fig. 8 shows that the IF signals track the RF input signal envelope and provides a variable supply voltage 'Vds' to the device for three distinct IF load conditions, each optimized for a different drain voltage, to realize both high efficiency and better linearity. For a supply voltage of 28V and V_{bias}=-2.05V, a drain efficiency of 43.5% was achieved with an output peak envelope power (PEP) of 39.72dBm.

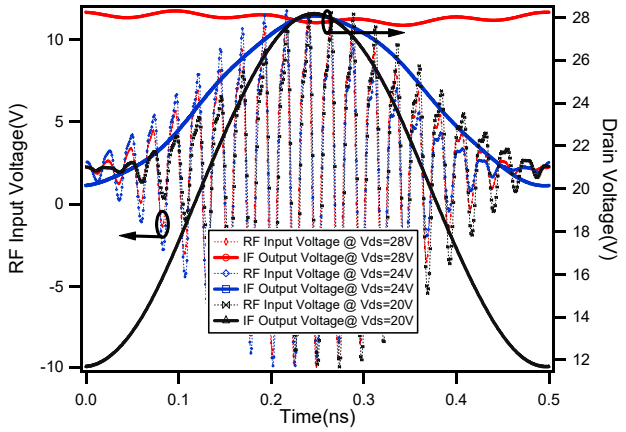

Fig. 8 Experimentally measured dynamic IF voltage envelops in-phase with input RF voltages for the three cases considered

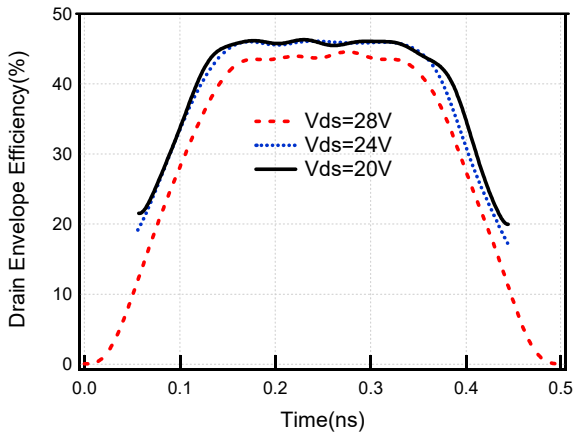

Fig. 9 Experimentally measure drain envelope efficiencies for three different cases at constant input drive and fixed bias level V_{bias}=-2.05V

The maximum drain envelope efficiency is achieved with a supply voltage of 24V; the maximum drain efficiency is 46.2% with an output PEP of 40.5dBm. However, a slightly better performance in terms of efficiency and output power was achieved with supply voltage of 20V. As a matter of fact, varying Vds greatly reduced the average power dissipation and increased the permissible peak output power, and thus enabled higher power efficiency than was possible with a fixed power supply voltage of 28V. Varying both Vds and the output power, greatly increased power efficiency (can be seen from Fig. 9, that is an envelope domain representation of efficiencies [10]) compared with using fixed voltage power supply.

It was observed that at Vds=20V, the IM3 and IM5 distortions are suppressed by 10dBc and 3dBc respectively as compared to the static Vds=28V where a short circuit impedance was maintained for all four IF components. In contrast to Vds=20V, it can be clearly seen from Table I, a slight improvement in IM3 distortions was observed at Vds= 24V whilst it showed 8dBc improvement in IM5 distortion products. These results, therefore, indicate that the injected optimum baseband signal significantly modify the levels of both IM3 and IM5 inter-modulation distortion products.

TABLE I
MEASURED LINEARITY RESULTS WITH THREE-TONE STIMULI

Supply Voltage(V)	IM5L dBc	IM3L dBc	W1 dBm	Wc dBm	W2 dBm	IM3H dBc	IM5H dBc
28	-35.68	-12.83	27.85	35.69	28.02	-13.12	-36.47
24	-43.05	-15.86	28.08	35.18	28.15	-16.37	-43.26
20	-38.95	-22.81	28.39	34.39	28.49	-22.57	-39.41

V. EMULATION OF CLASS J

To further demonstrate the enhanced broadband load-pull capabilities of the measurement system, a class-J mode was emulated by presenting established impedances [20] at the device package plane. The device was deep class-AB biased, and driven approximately 2dB into compression with a two-tone modulated excitation centered at 2GHz with a 4MHz tone spacing. An optimum reactive fundamental impedance was presented to all fundamental tones and a suitably phased reactive second harmonic impedance termination was presented to the tones around the 2nd harmonic. The third harmonic components were terminated arbitrarily.

This analysis was specifically designed to investigate the effectiveness of baseband linearization techniques for novel PA modes and architectures, so as in the previous analysis, the impedance presented to all baseband tones was swept over a measurement around the short circuit condition. Selected inter-modulation distortion (IMD) contours are plotted in Fig. 10, which in this case show an interesting result – there are different non-real optima for different IMD terms. The optimum $IM3_L$ and $IM3_H$ baseband termination is found to be -43.2dBc and -45.5dBc respectively, and is approximately 18.5dBc better than the case where usual short circuit is provided to all the significant baseband components. However, from the IM5 point of view, the optimum $IM5_L$ and $IM5_H$ showed the minimum distortion products which were found to be -59.3dBc and 61.1dBc respectively. The ability of the system to maintain broadband baseband, fundamental and

second harmonic loads is critical. This capability is evident in Fig. 10 where the second and fundamental loads for all 40 baseband points are overlaid on the same smith chart. The variation and dispersion in these loads can be seen to be minimal and in terms of normalized Cartesian coordinates, this was measured to be in the region of 0.6% (1Standard Deviation) for both fundamental and second harmonic loads. A reduction of approximately 18.5dBc in IM3 was observed, albeit at the expense of significant increase in $IM5_L$ of approximately 16 dB. Conversely, analysis showed that whilst maintaining the optimum impedance for IM5, there was an 8dBc performance reduction in IM3.

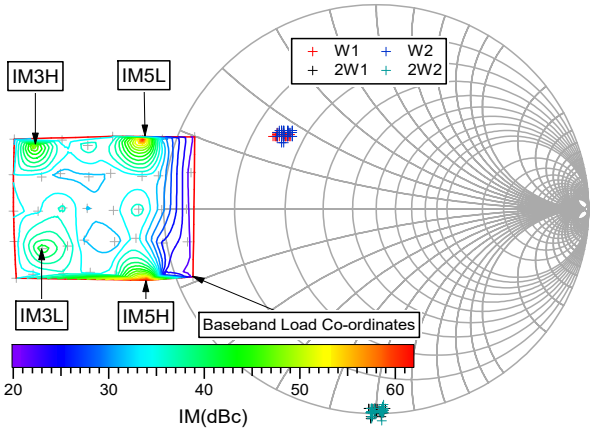

Fig. 10 Experimentally measured IM linearity contours as a function of IF reflection coefficient (Γ_L) for a class-J emulated RF impedance environment

Fig. 11 shows the baseband voltage waveforms that resulted when the IF impedances for the best IM3 linearity were presented to the device. The magnitude of both waveforms is almost indistinguishable but there is an apparent phase shift. The improvement in IM3 worsens with the increased baseband voltage. The IM5 voltage waveforms for best linearity are not plotted here for simplicity and are almost identical in shape to IM3 waveforms.

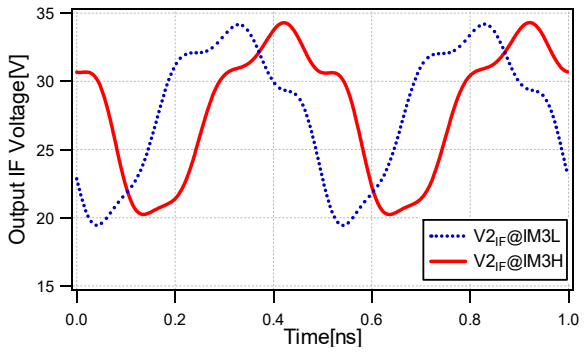

Fig. 11 Experimentally measured baseband voltages that resulted for the best IM3 linearity performance under class-J mode of operation

VI. Conclusions

The capability of the modified modulated waveform measurement system has been demonstrated that allows the emulation of novel PA modes and architectures, including for example class-J and envelope tracking respectively. The linearity investigations of a 10W GaN HEMT under different modulation excitations showed that the optimum impedance for best linearity lies outside the Smith chart. Interestingly, the results also suggest that there exists separate resistive optimum impedance for suppression of IM3 and IM5 distortion products when RF components are terminated with nominal 50Ω impedance. Additionally, the ET measurements showed that efficiency as well as linearity improves at reduced drain supply voltages. Average drain efficiency of 41.78%, at an output PEP of 40.43dBm was achieved whilst giving an improvement of 3.48% in efficiency and 10dBc in IM3 when compared to the static Vdc, where a short circuit impedance was maintained for all four baseband components.

The true benefit of this enhanced system becomes apparent through the broadband emulation of a class-J mode of operation however, where initial results suggest that there exist separate reactive optimum impedances for suppression of IM distortion products, and this key observation may have significant implications for modern broadband PA design approaches [21], [22].

Acknowledgment

The author would like to profusely thank Jonathan Lees, Johannes Benedikt, and Paul Tasker for their incessant support to carry out this research work at the Agilent Centre for High Frequency Engineering, Cardiff School of Engineering, Cardiff University, United Kingdom. The author further would like to thank CREE for supplying the devices and Mesuro for providing access to Tektronix Arbitrary Waveform Generator (AWG).

References

[1] Joel Vuolevi and Timo Rahkonen, *Distortion in RF Power Amplifiers*, Norwood, MA: Artech House, 2003.
[2] B. Kenington, *High-Linearity RF Amplifier Design*, Norwood, MA: Artech House, 2000.
[3] C. Fan and K. M. Cheng, "Theoretical and experimental study of amplifier linearization based on harmonic and baseband signal injection technique," *IEEE Trans. Microwave Theory Tech.*, vol. 50, pp. 1801–1806, July 2002.
[4] J. Vuolevi, J. Manninen, T. Rahkonen, "Cancelling the memory effects in RF power amplifiers", *IEEE International Circuits and Systems Symposium*, 2001, pp. 57–60.
[5] S. C. Cripps, *Advanced Techniques in RF Power Amplifier Design*, Norwood, MA, Artech House, 2006.
[6] M. D. LeFevre, D. W. Runton, C. T. Burns, M. K. Mellor, "Digital Predistortion from an RF Perspective", *2010 IEEE Topical Symposium on Power Amplifiers for Wireless Communications*, September 2010.
[7] Z. Yusoff, J. Lees, P. J. Tasker, J. Benedikt, S.C. Cripps, "Linearity Improvement in RF Power Amplifier System Using Integrated Auxiliary Envelope Tracking System", *in Proc. of IEEE MTT-S International*, June 2011, pages: 1 -4.
[8] A. Alghanim, J. Benedikt, P.J. Tasker, P "A measurement test-set for characterisation of high power LDMOS transistors including memory effects" *Proceedings of High Frequency Postgraduate Student Colloquium*, 5-6 September 2005 Page(s): 29 – 32.

[9] A. Alghanim, J. Lees,T. Williams, J. Benedikt, P.J. Tasker, "Using active IF load-pull to investigate electrical base-band induced memory effects in high-power LDMOS transistors," in Proc. Asia-Pacific Microwave Conference, 2007, 11-14 Dec. 2007 Page(s):1 - 4.
[10] J. Lees, T. Williams, S. Woodington, P. McGovern, S. Cripps, J. Benedikt, and J. Tasker, "Demystifying Device related Memory Effects using Waveform Engineering and Envelope Domain Analysis," *European Microwave Conf.*, Oct. 2008, Amsterdam, pp:753-756.
[11] A. Alghanim, J. Lees,T. Williams, J. Benedikt, P.J. Tasker, P "Using active IF load-pull to investigate electrical base-band induced memory effects in high-power LDMOS transistors," *Proceedings of Asia-Pacific Microwave Conference*, December 2007, Page(s):1 - 4.
[12] M. Akmal, J. Lees, S. Bensmida, S. Woodington, J. Benedikt, K. Morris, M. Beach, J. McGeehan, P. J. Tasker, " The Impact of Baseband Electrical Memory Effects on the Dynamic Transfer Characteristics of Microwave Power Transistors", in Proc. of *4th International Nonlinear Microwave Monolithic Integrated Circuit(INMMIC)*, April 2010, pages: 148 – 151.
[13] T. Williams, J. Benedikt, P. J. Tasker, "Fully Functional Real Time Non-Linear Device Characterization System Incorporating Active Load Control", *in Proc. 36th European Microwave Conference (EuMC)*, October 2006, pages: 1610-1613.
[14] T. Williams, J. Benedikt, P. J. Tasker, "Experimental evaluation of an active envelope load pull architecture for high speed device characterization", in Proc. *IEEE MTT-S Int. Microwave Symp. Dig*., Long Beach, June 2005, pages: 1509-1512.
[15] M. Akmal, J. Lees, S. Bensmida, S. Woodington, V. Carrubba, S. Cripps, J. Benedikt, K. Morris, M. Beach, J. McGeehan, P. J. Tasker, "The Effect of Baseband Impedance Termination on the Linearity of GaN HEMTs", *40th IEEE European Microwave Con*ference(EuMC), September 2010, pages: 1046 -1049.
[16] M. Akmal, J. Lees, V. Carrubba, S. Bensmida, S. Woodington, J. Benedikt, K. Morris, M. Beach, J. McGeehan, P. J. Tasker, "Minimization of Baseband Electrical Memory Effects in GaN HEMTs Using IF Active Load-pull", *in Proc. Of IEEE Asia Pacific Microwave Conference (APMC*. December 2010*)*, pages: 5-8.
[17] M. Akmal, V. Carrubba, J. Lees, S. Bensmida, S. Woodington, J. Benedikt, K. Morris, M. Beach, J. McGeehan, P. J. Tasker, "Linearity Enhancement of GaN HEMTs under Complex Modulated Excitation by Optimizing the Baseband Impedance Environment", in Proc. of *IEEE MTT-S International. Microwave Sympo*sium, June 2011, pages(s):1-4.
[18] M. Akmal, J. Lees, , J. Benedikt, P.J. Tasker, Characterization of electrical memory effects for complex multi-tone excitations using broadband active baseband load-pull", in *Proc. of 42nd European Microwave Conference (EuMC)*, October 2012, pages: 1265 -1268.
[19] Chaudhary, M.A.; Lees, J.; Benedikt, J.; Tasker, P., "Reduction of baseband electrical memory effects using broadband active baseband load-pull", *in Proc. of IEEE Internation Wireless Symposium (IWS)*, April 2013, pages: 1 - 4.
[20] P. Wright, J. Lees, P. J. Tasker, J. Benedikt, S.C. Cripps, "An efficient, linear, broadband class-J-mode PA realised using RF waveform engineering", *in Proc. of IEEE MTT-S International*, June 2009, pages: 653 -656.
[21] V. Carrubba, A. L. Clarke, M. Akmal, J. Lees, J. Benedikt, P. J. Tasker, S. C. Cripps, "On the Extension of the Continuous Class-F Mode Power Amplifier," *IEEE Trans. Microw, Theory and Tech.,* vol. 59, March 2011, pp. 1294-1303.
[22] V. Carrubba, J. Lees, J. Benedikt, P. J. Tasker, S. C. Cripps, "A Novel Highly Efficient Broadband Continuous Class-F RFPA Delivering 74% Average Efficiency for an Octave Bandwidth," *Proceeding of the IEEE MTT-S Dig*., June 2011, pages: 1 – 4.

Muhammad Akmal Chaudhary (M'09–SM'15) received the Ph.D. degree in Electrical Engineering from Cardiff University, United Kingdom, in 2011. He is currently working as an assistant professor at the Department of Electrical Engineering, Ajman University of Science & Technology, Ajman, United Arab Emirates. Prior to this position, he was a Postdoctoral Research Associate between October 2011 and September 2012 at the Agilent Centre for High Frequency Engineering, Cardiff School of Engineering, Cardiff University, United Kingdom.

From January 2005 to September 2006, he worked with Alcatel-Lucent Pakistan as a Technical Support Engineer, Lahore, Pakistan, where he was involved in the maintenance, troubles shooting and all the major operational applications of Alcatel 1000 E 10 MM a high capacity Network Switching subsystem (NSS).

He has authored and co-authored over 40 peer reviewed scientific papers. His research interests are developing the multi-tone waveform measurement system, characterization of nonlinear distortion in microwave power transistors, investigations of memory effects, and multi-tone measurements of high-power and spectrum-efficient RF power amplifiers.